ENVIRONMENTAL RESEARCH
LETTERS

OPEN ACCESS

RECEIVED
7 December 2022

REVISED
16 January 2023

ACCEPTED FOR PUBLICATION
7 February 2023

PUBLISHED
24 February 2023

LETTER

Increased floodplain inundation in the Amazon since 1980

Ayan S Fleischmann[1,2,*], Fabrice Papa[3,15], Stephen K Hamilton[4,13], Alice Fassoni-Andrade[15], Sly Wongchuig[5], Jhan-Carlo Espinoza[14], Rodrigo C D Paiva[2], John M Melack[6], Etienne Flet-Chouinard[7], Leandro Castello[8], Rafael M Almeida[9], Marie-Paule Bonnet[10], Luna G Alves[11], Daniel Moreira[16], Dai Yamazaki[12], Menaka Revel[12] and Walter Collischonn[2]

1 Mamirauá Institute for Sustainable Development, Tefé, Brazil
2 Hydraulic Research Institute (IPH), Federal University of Rio Grande do Sul (UFRGS), Porto Alegre, Brazil
3 Laboratoire d'Etudes en Géophysique et Océanographie Spatiales (LEGOS), Université Toulouse, IRD, CNRS, CNES, UPS, Toulouse, France
4 Cary Institute of Ecosystem Studies, Millbrook, NY 12545, United States of America
5 University Grenoble Alpes, IRD, CNRS, Grenoble INP, IGE, 38000 Grenoble, France
6 Earth Research Institute, University of California, Santa Barbara, United States of America
7 Department of Environmental Systems Science, Institute for Atmospheric and Climate Science, ETH Zurich, Zurich, Switzerland
8 Department of Fish and Wildlife Conservation, Virginia Polytechnic Institute and State University, Blacksburg, VA, United States of America
9 School of Earth, Environmental, and Marine Sciences, The University of Texas Rio Grande Valley, Edinburg, TX 78539, United States of America
10 Espace-DEV-Research Institute for Development (IRD), Univ Montpellier, Montpellier, France
11 Geological Survey of Brazil (SGB), Belo Horizonte, Brazil
12 Institute of Industrial Science, The University of Tokyo, 4-6-1, Komaba, Meguro-ku, Tokyo 153-8505, Japan
13 Kellogg Biological Station, Michigan State University, Hickory Corners, MI 49060, United States of America
14 Institut des Géosciences de l'Environnement, Université Grenoble Alpes, IRD, CNRS, 70 Rue de la Physique. Domaine Universitaire, Saint Martin d'Hères 38400, France
15 Institut de Recherche pour le Développement (IRD), Institute of Geosciences, Campus Universitário Darcy Ribeiro, Universidade de Brasília (UnB), Brasília, DF 70910-900, Brazil
16 Geological Survey of Brazil (SGB), Géosciences Environnement Toulouse (GET), Toulouse, France
* Author to whom any correspondence should be addressed.

E-mail: ayan.fleischmann@gmail.com

Keywords: climate change, wetlands, remote sensing, connectivity, Amazon River basin

Supplementary material for this article is available online

Abstract

Extensive floodplains throughout the Amazon basin support important ecosystem services and influence global water and carbon cycles. A recent change in the hydroclimatic regime of the region, with increased rainfall in the northern portions of the basin, has produced record-breaking high water levels on the Amazon River mainstem. Yet, the implications for the magnitude and duration of floodplain inundation across the basin remain unknown. Here we leverage state-of-the-art hydrological models, supported by *in-situ* and remote sensing observations, to show that the maximum annual inundation extent along the central Amazon increased by 26% since 1980. We further reveal increased flood duration and greater connectivity among open water areas in multiple Amazon floodplain regions. These changes in the hydrological regime of the world's largest river system have major implications for ecology and biogeochemistry, and require rapid adaptation by vulnerable populations living along Amazonian rivers.

1. Introduction

The seasonal flood pulse of the Amazon River, the Earth's largest river system, dictates the ecological structure and function of its floodplains and the ecosystem services they support (Junk *et al* 1989, Melack and Coe 2021). The composition, productivity, and life cycles of river and floodplain biota are adapted to seasonal flood regimes (Junk *et al* 1989), including fisheries underpinning human food and income security. The fertile floodplains provide food and fiber to support human communities across the basin (Sherman *et al* 2016, Langill and Abizaid 2020, Fleischmann 2021). These vast floodplains influence climate (Paiva et al 2011, Santos et al 2019) and carbon cycling within and beyond the Amazon basin, and are hotspots for greenhouse gas emissions (Richey et al 2002, Melack et al 2004, Abril et al 2014, Pangala et al 2017). Changes to the Amazon basin's flooding regime can therefore produce unprecedented impacts from local to global scales.

The Amazon River system is increasingly affected by multiple stressors (Castello et al 2013). Changes in regional climate have been superimposed on human disturbances such as construction of dams (Chaudhari and Pokhrel 2022) and deforestation in both uplands (Costa et al 2003) and floodplains (Renó et al 2011). Based on river gage measurements, recent studies have shown higher maximum water levels in the Amazon since the late 1990s (Gloor et al 2013, Barichivich et al 2018), linked to a ∼17% increase in wet-season rainfall over the northern part of the basin (north of 5° S) from 1981 to 2017 (Espinoza et al 2019a, Haghtalab et al 2020, Funatsu et al 2021). This change has been hypothesized to be driven by changes in sea surface temperature in both the Pacific and Atlantic oceans (Marengo and Espinoza 2016, Friedman et al 2021) and the consequent strengthening of the Walker and Hadley circulation (Barichivich et al 2018, Espinoza et al 2019a, Friedman et al 2021).

Increased rainfall in the northern Amazon basin has resulted in higher river water levels and discharges along the mainstem Amazon River (figure 1(a)) (Heerspink et al 2020). Seven of the ten highest maximum annual water levels recorded in the last 119 years at Manaus (Negro-Amazon confluence) have occurred since 2009 (figure 1), including the highest-ever recorded water level in June 2021, which affected more than 500 000 people in the Amazonas State of Brazil (Espinoza et al 2022). This contrasts with a prevailing perception by the public and many scientists that the Amazon is drying out, influenced by the well-publicized decrease in rainfall and streamflow in southern Amazon sub-basins, a trend that has also been linked to changes in ocean-atmosphere interactions (Espinoza et al 2019a).

While trends in water levels are readily apparent from gages along major rivers, understanding their impacts on ecological and biogeochemical processes and human communities requires quantifying how higher water levels translate into commensurate increases in flooding extent and duration, as well as hydrological connectivity of seasonally inundated floodplain areas, which have not yet been analyzed. Here, we use hydrological-hydrodynamic models (MGB (Siqueira et al 2018) and CaMa-Flood (Yamazaki et al 2011)) and long-term satellite-derived datasets (see section 2), supported by *in-situ* observations, to analyze for the first time a 40 year record of floodplain inundation patterns in relation to basin-wide rainfall changes.

2. Methods

2.1. Dynamic inundation from hydrological models

Monthly inundation estimates were obtained from two state-of-the-art hydrological-hydrodynamic models—MGB (Siqueira et al 2018) and CaMa-Flood (Yamazaki et al 2011). MGB has been used to investigate Amazon hydrological processes (Paiva et al 2013, Sorribas et al 2016, 2020, Fleischmann et al 2020). It is a rainfall-runoff model coupled to a physically-based hydrodynamic routine developed to represent the river-floodplain interactions in large basins (Pontes et al 2017). The version used here is the same one developed for the entire South American continent (Siqueira et al 2018), and was validated against extensive *in-situ* and satellite data. Within the model, the river drainage network is divided into 15 km river reaches, for which unit-catchments are defined. While the input rainfall data has a daily time step, the model runs with an adaptive time step to maintain model stability (Neal et al 2012). The model was manually calibrated aiming at river discharge simulation, defining parameters for hydrologically homogeneous areas based on lithology/geology information and the boundaries of large South American basins. Multiple hydrological components (water levels, total water storage and evapotranspiration) were validated based on *in-situ* and satellite data, showing a satisfactory model performance across the Amazon region (Siqueira et al 2018). In turn, CaMa-Flood is a global hydrodynamic model (Yamazaki et al 2011) that uses equations similar to MGB to simulate river-floodplain processes (Bates et al 2010, Yamazaki et al 2013). Here we use the same version as available in the eartH2Observe platform (www.earth2observe.eu) (Schellekens et al 2017). The model is forced with HTESSEL model runoff fields, with a 0.25° spatial resolution and 1 h time step. In both MGB and CaMa-Flood, the river channels are considered as rectangular cross sections, and the floodplains are assumed as storage units, so that no flow occurs along floodplains. Both MGB and CaMa-Flood models use daily MSWEP v 1.1 rainfall (Beck et al 2017) and provide daily inundation extent at 500 m resolution for the period 1980–2014.

The adopted model versions simulate the Amazon basin in its natural scenario, i.e. without anthropogenic alterations such as dams. The models' ability to simulate inundation extent along Amazon floodplains was recently assessed by Fleischmann et al (2022). In addition to inundation extent, we also assess the flood storage estimates with both models, given their satisfactory capability to estimate both inundation and water depth across the basin (Yamazaki et al 2011, Paiva et al 2013, Siqueira et al 2018). The long-term maximum inundation area (including open water of river channels) over the Amazon mainstem floodplain between the cities of

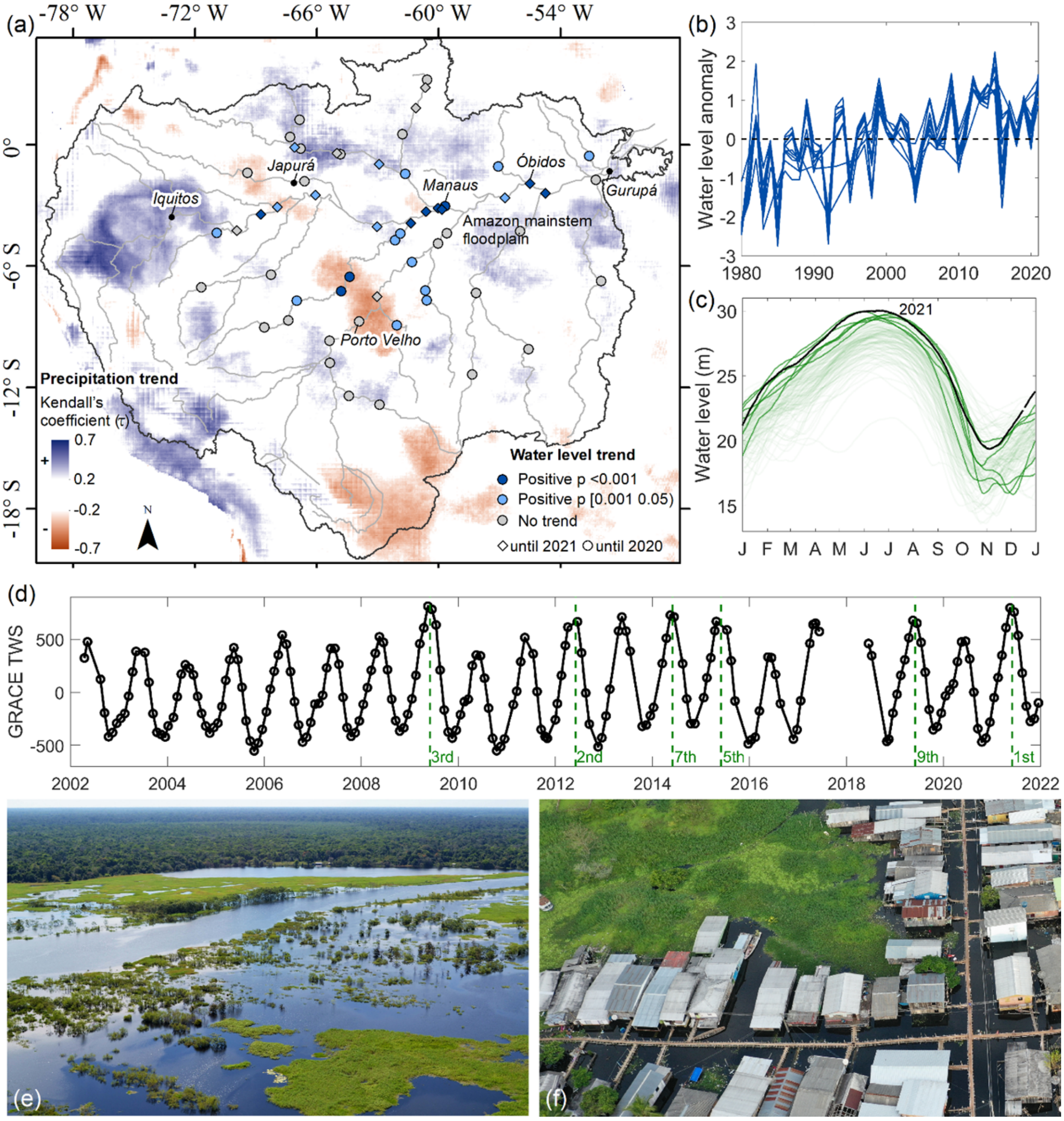

Figure 1. The increasing magnitude of Amazon floods. (a) Map depicting areas of significant trends of annual rainfall (background colors) and annual maximum water levels at 58 *in-situ* gages (circles) across the Amazon River basin. Blue and orange show areas of strong monotonic positive and negative trends over 40 years, respectively (Mann-Kendall test). River level gages (circles) are colored according to the significance of their long-term trends. (b) Anomalies relative to the mean of the annual maximum water levels for 12 gages along the Amazon mainstem from 1980–2021; the individual series are presented in figure S1. (c) Time-series of daily river levels for each of the 119 years of record at the Manaus gage on the lower Negro River, indicative of the level of central Amazon River. The years with the seven exceptional floods observed since 2009 are highlighted in dark green and black. (d) Monthly series of total water storage (mm) for the Amazon river-floodplain system between the cities of Iquitos (Loreto, Peru) and Gurupá (Pará, Brazil). Vertical dashed lines refer to the same years highlighted with dark green lines in figure (c). The rank of the 10 highest annual maximum water levels in the 119 year record is noted next to each vertical line; before 2009, the other extreme years were 1953 (4th largest), 1976 (6th), 1989 (8th), and 1922 (10th). Photos in (e), (f) show the recent extreme floods of 2012 at Mamirauá Reserve, and 2021 in Manacapuru, with flooded streets along the city's urban area. Photo courtesy by João Paulo Borges Pedro. Photo courtesy by Maycon Castro.

Iquitos and Gurupá is estimated to be 118 500 km^2 and 115 000 km^2 for CaMa-Flood and MGB, respectively, which are close to the estimate by Hess *et al* (2015) of 115 800 km^2, which in turn is widely considered as the benchmark for Amazon wetland mapping (Fleischmann *et al* 2022). The Amazon mainstem floodplain area was delineated considering the flood mask by Hess *et al* (2015), and includes the lower reaches of major tributaries (see area in figure 1).

2.2. Open water remotely-sensed data

Long-term remote sensing observations of non-vegetated, open water extent are scarce. Here we use the high-resolution (30 m) Global Surface Water Occurrence (GSWO) product (available at <https://global-surface-water.appspot.com/download>) (Pekel *et al* 2016), which is based on classification of the entire archive of the Landsat 5 Thematic Mapper, the Landsat 7 Enhanced Thematic Mapper-plus and the Landsat 8 Operational Land

Imager orthorectified images, covering the period 1985–2020. Given the inability of optical imagery to sense inundation obscured by dense vegetation (Aires *et al* 2018, Zhou *et al* 2021), it is only capable of monitoring open water areas or sparsely vegetated inundated areas. Its applicability for the Amazon floodplain region is restricted to areas with extensive lakes. Thus, the lower river reaches, mainly downstream of the Negro-Amazon river confluence, are suitable for the use of GSWO. In upper reaches, inundated forests are more common, although floodplain lakes bordered with non-forest vegetation are present and are used to assess long-term changes. Besides being in agreement with the other inundation datasets and the increasing trend for water levels across the Amazon River (figure 3), the ability of GSWO to represent open water inundation changes was considered satisfactory given its correlation with the *in-situ* water levels in the Amazon River at Óbidos gage (figure S5(a)), which shows the high agreement between annual maxima of *in-situ* water level measurements and annual maxima of inundation area ($R = 0.81$, $P < 0.001$). The GSWO version used here is provided at a monthly basis and converted to annual maximum and minimum maps to reduce the uncertainties related to lack of images due to cloud-cover, especially during wet season.

2.3. Ancillary data

Rainfall data from CHIRPS v2.0 (Funk *et al* 2015) at 0.05° spatial resolution, which adequately represent the Amazon basin's regime (Wongchuig Correa *et al* 2017, da Motta Paca *et al* 2020, Haghtalab *et al* 2020, Funatsu *et al* 2021, Espinoza *et al* 2022), were used to assess long-term trends and interannual variability across the basin. Total water storage data from GRACE (April 2002–June 2017) and GRACE-FO (January 2018-today) missions (Tapley *et al* 2004, Landerer *et al* 2020), based on the JPL RL06M Mascon solution, were used to investigate the impact of extremely wet years on seasonal water storage in the central Amazon. Given its short-term data availability (since 2003) and coarse resolution (∼300 km), no long-term trend analysis was performed, but the GRACE data were used to infer large-scale water storage patterns. *In-situ* observations of river water levels were obtained from the Brazil's National Water Agency for all gages in the Brazilian Amazon basin, in addition to *in-situ* data from the Peru's SENAMHI for the Tamshiyacu gage on the Amazon River close to the city of Iquitos. Because of delayed data availability, at the time of this study some gages did not yet have data available for the 2021 extreme flood event that occurred in central Amazon (Espinoza *et al* 2022); the gages which data covered the 2021 flood are highlighted in figure 1(a).

The linear model developed by Hamilton *et al* (2002) was used as an additional independent estimate of inundation extent. It is based on passive microwave emission data from the Scanning Multichannel Microwave Radiometer (spatial resolution of 0.25°) and *in-situ* data from the Manaus river gage. Here, we used the aggregated time series of inundation extent for the entire mainstem Amazon floodplain from Hamilton *et al* (2002) (see their figure 1). It is important to notice that the linear model was developed for a water level range slightly smaller than the one assessed here (the maximum water level used was 28.9 m, while the 2021 flood reached 30 m).

2.4. Trend analysis

Maximum and minimum annual inundation trends obtained from MGB (1980–2014), CaMa-Flood (1980–2014) and GSWO datasets (1984–2020) were analyzed individually without any type of merging, and spatially mapped with the rank-based non-parametric Mann Kendall trend test (Kendall and Gibbons 1975) at the product resolution (500 m for MGB and CaMa-Flood and 30 m for GSWO), i.e. for each pixel the trend was assessed considering the entire inundation time series. The long-term changes in annual maximum and minimum flooded areas, as well as annual amplitudes (i.e. annual maxima minus minima), for the Amazon mainstem floodplain were obtained by applying a linear fit to the annual series, and then computing the change between the inundation in the first and last years of the adjusted line. Step changes in the slopes of the time series were evaluated using the non-parametric approach to the change-point problem (Pettitt 1979), which yields the year in which the largest step change occurs in the whole series.

The annual maximum inundation extent was averaged for the decades 1985–1996 and 2009–2020 for the entire Amazon River floodplain between the cities of Iquitos and Gurupá. These two decades were chosen as representative of 12 years of recent (2009–2020) and earlier (1985–1996) inundation regimes, given the first year of GSWO availability (1985). The year 1996 has been identified as the beginning of a change in the rainfall regime, as recently reported (Espinoza *et al* 2019a). The year 2021 was not considered since it was not available in GSWO or with the hydrological models. In the case of the models, data were only available until 2014 because the model forcings (i.e. rainfall and runoff) did not extend to more recent years. Although updated versions of the models are available until present time with different model forcings than those used in the consolidated versions, the new runs do not satisfactorily represent the water level trends across central Amazon due to unsatisfactory bias correction, and thus are unsuitable to assess inundation trends (Yamazaki, pers. comm.; Brêda, pers. comm.). Given the unsuitability of GSWO for forested floodplains and issues with cloud cover, only MGB and CaMa-Flood were used to estimate the long-term changes in inundation extent for the entire Amazon mainstem floodplain. GSWO was only used to assess flood duration and open water lateral connectivity along floodplain open water areas in the lower Amazon downstream of Manaus. Finally, besides inundation, we assess flood storage trends (including all surface water) with both the MGB and CaMa-Flood models, following the same methodology adopted for the assessment of inundation extent.

2.5. Open water lateral connectivity

Open water lateral connectivity and flood duration changes were computed over the 1985–1996 and 2009–2020 decades with the GSWO dataset for the lower Amazon floodplain between Manaus and Gurupá, which is characterized by an abundance of large lakes (Sippel *et al* 1992). To estimate connectivity changes, we used the methodology presented by Trigg *et al* (2013). This analysis estimates, for a given floodplain area, the degree of connectivity across a given direction, measured as the number of pixel pairs connected across a given distance. The direction adopted for each analyzed area refers to the longest dimension of the floodplain unit, e.g. west-east for the Curuai floodplain (figure 3(b)). For the flood duration changes, long-term maps (i.e. estimation of how many days per year a given pixel was, on average, inundated) were computed for the decades 1985–1996 and 2009–2020, and subtracted from each other. The use of a full decade diminishes the uncertainties related to data unavailability in specific months due to cloud cover in GSWO.

3. Results

3.1. Recent increases in rainfall, river water levels and total water storage

Long-term records reveal that annual rainfall has increased in certain regions of the Amazon basin, while in others it has decreased (figure 1(a)) (Barichivich *et al* 2018, Espinoza *et al* 2019a). At the scale of the entire basin, the influence of areas with increased rainfall outweighs the counteracting influence of areas with decreased rainfall. Trends in annual maximum river levels show increases in several major tributaries and along the mainstem Amazon River (figure 1(b)). Positive, statistically significant trends for both annual maximum water levels and water level amplitudes (i.e. annual maxima minus minima) are observed for the mainstem Amazon (figure 1(c)), Negro and Purus rivers, and in lower reaches of other major tributaries subject to backwater effects from the mainstem Amazon (figures 1(a) and S2). Along the lower mainstem region (at the Óbidos gage station), where the largest increase is observed, the average maximum water level has risen by 87 cm (13% of the mean annual amplitude of ~6.90 m, computed for the period 2009–2021) between 1985–1996 and 2009–2021. These periods refer to the earliest and latest multi-year periods available from the GSWO dataset. In contrast to maximum water levels, annual minima along the central Amazon have remained unchanged over the past 40 years (figure S2). The decrease in rainfall in parts of the southern basin coincides with a negative trend of annual minimum discharge documented in the upper Madeira River (at the Porto Velho gage station), which includes the extensive Llanos de Moxos wetlands along the Mamoré River (Espinoza *et al* 2019b).

Additional evidence for temporal changes in floodplain water storage, although over a shorter period, is provided by the total water storage variation along the central Amazon floodplains estimated from gravity field variations by the GRACE and GRACE-FO satellite missions since 2002 (figure 1(d)). An increase in total water storage for individual flood events has been previously shown for the Amazon (Chen *et al* 2010), but our analysis for the entire 2003–2021 period supports the role of floodplain inundation dynamics in the seasonal and interannual changes of water storage at the regional scale.

3.2. Patterns of increased inundation along the Amazon mainstem

Our analysis shows that the change in rainfall has not only increased water levels, as stressed by previous studies, but also the annual maximum inundation extent in the floodplains along the Amazon River mainstem (figure 2(a)). In the Amazon mainstem floodplains between the cities of Iquitos (Peru) and Gurupá (Brazil) (figure 1(a)), hydrological models suggest that the annual maximum inundation extent increased by 26% (93 000–117 000 km^2 between 1980 and 2014, with an annual increase of approximately 700 km^2 yr^{-1}, P-value < 0.001). In contrast, annual minimum inundation extent has not changed over the same period (figure S3). As a result, the inundation amplitude (annual maximum minus minimum inundated area) has increased (trends of 600–700 km^2 yr^{-1}; P-value < 0.001; figure S3).

The modeled annual maximum inundation area in Amazon mainstem floodplains has the same step change observed for rainfall in the northern Amazon (Espinoza *et al* 2019a) in 1998 (P-value $= 0.02$ for MGB and P-value $= 0.001$ for CaMa-Flood models), increasing by 12% from a mean of 98 000 km^2 for the period 1980–1998 to a mean of 110 000 km^2 for 1999–2014. Furthermore, the modeled increase in maximum inundation extent and water levels translates into increased surface water storage (figure S4), consistent with trends in total water storage derived from GRACE satellite observations (figure 1(d)), further supporting the hydrological models.

Increased inundation as revealed by hydrological models is corroborated by independent satellite observations, both by passive microwave-based measurements for the central Amazon (figure S5(b); Hamilton *et al* (2002)), and by the Landsat-based GSWO. However, the increased inundation observed

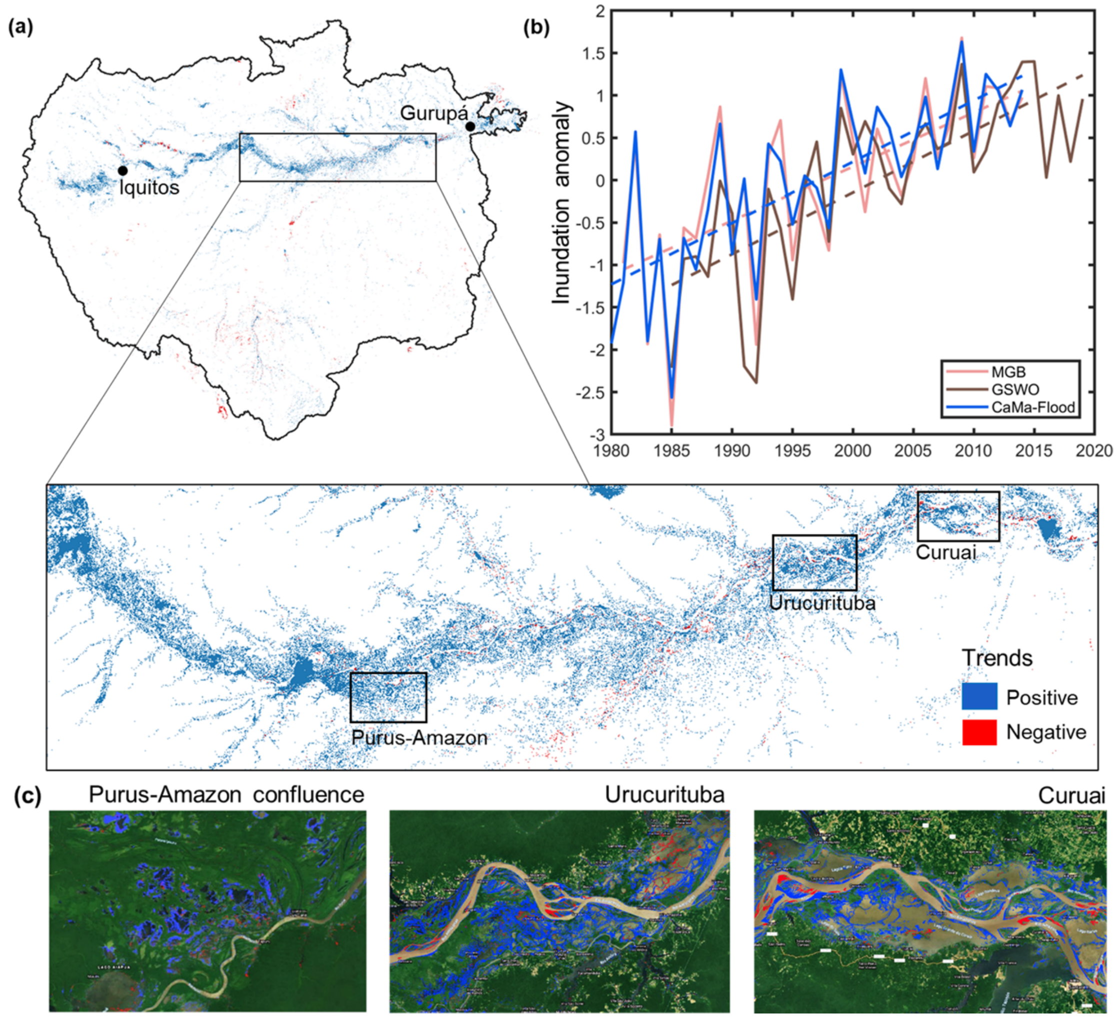

Figure 2. Large-scale increase of inundation extent over the Amazon River floodplain. (a) Spatial assessment of inundation trends over the Amazon basin based on the combination of two hydrodynamic models (500 m spatial resolution) and Landsat satellite (30 m) observations of open-water area, showing areas with positive (blue) and negative (red) trends over 1985–2020 based on Mann-Kendall tests. Here, the three datasets are plotted together; individual maps are presented in figure S8. (b) Anomalies (deviations from the long-term mean) of maximum annual inundation extent for the entire Amazon mainstem floodplain between the cities of Iquitos and Gurupá, depicting long-term trends, based on the two hydrological models and GSWO. (c) Spatial trends in open-water area in the three floodplain subregions delineated in figure (a) based on the Landsat satellite observations. Areas with null color have no significant trend, and are associated either with pixels that are always (such as central areas of lakes) or never flooded.

by GSWO over 1985–2020 is restricted to floodplain areas dominated by open water, which exist mainly downstream of Manaus (figures 2(c) and S6), because Landsat cannot detect inundation beneath dense canopies of flooded forest or floating herbaceous vegetation, in contrast to the two hydrological models. Additionally, a few areas with decreasing inundation trends are associated with natural sediment accumulations along newly formed islands and crevasse splay formations within floodplains (see detail in figure 3(a)).

In addition to increased inundated area, GSWO data indicate that flood duration (i.e. the average number of days that a pixel is subject to flooding in a given year) increased in 65% between the cities of Manaus and Monte Alegre (13 300 out of 20 400 km^2; excluding lake surfaces permanently flooded) between the decades of 1986–1995 and 2009–2020 (figures 3(a) and S7(a)). Some of the increases in duration were large, with 23% of the area subject to inundation changes being flooded for an additional 50 or more days per year across the two decades (figure S7(a)). The total open water area subject to inundation for more than 180 days per year has increased by 14% for the whole floodplain between Manaus and Monte Alegre (from 16 300 to 18 600 km^2; figure S7(b)).

Because of more extensive and longer flooding, connectivity among floodplain waterbodies and with the main channels has increased in many places along the Amazon floodplain (figure 3(b)). This is revealed by GSWO for open water areas downstream of Manaus. The largest impact on connectivity is observed in the Maracu and Camapu areas, with connected area within a 10 km distance increasing fivefold (figure 3(b)). A smaller yet notable increase

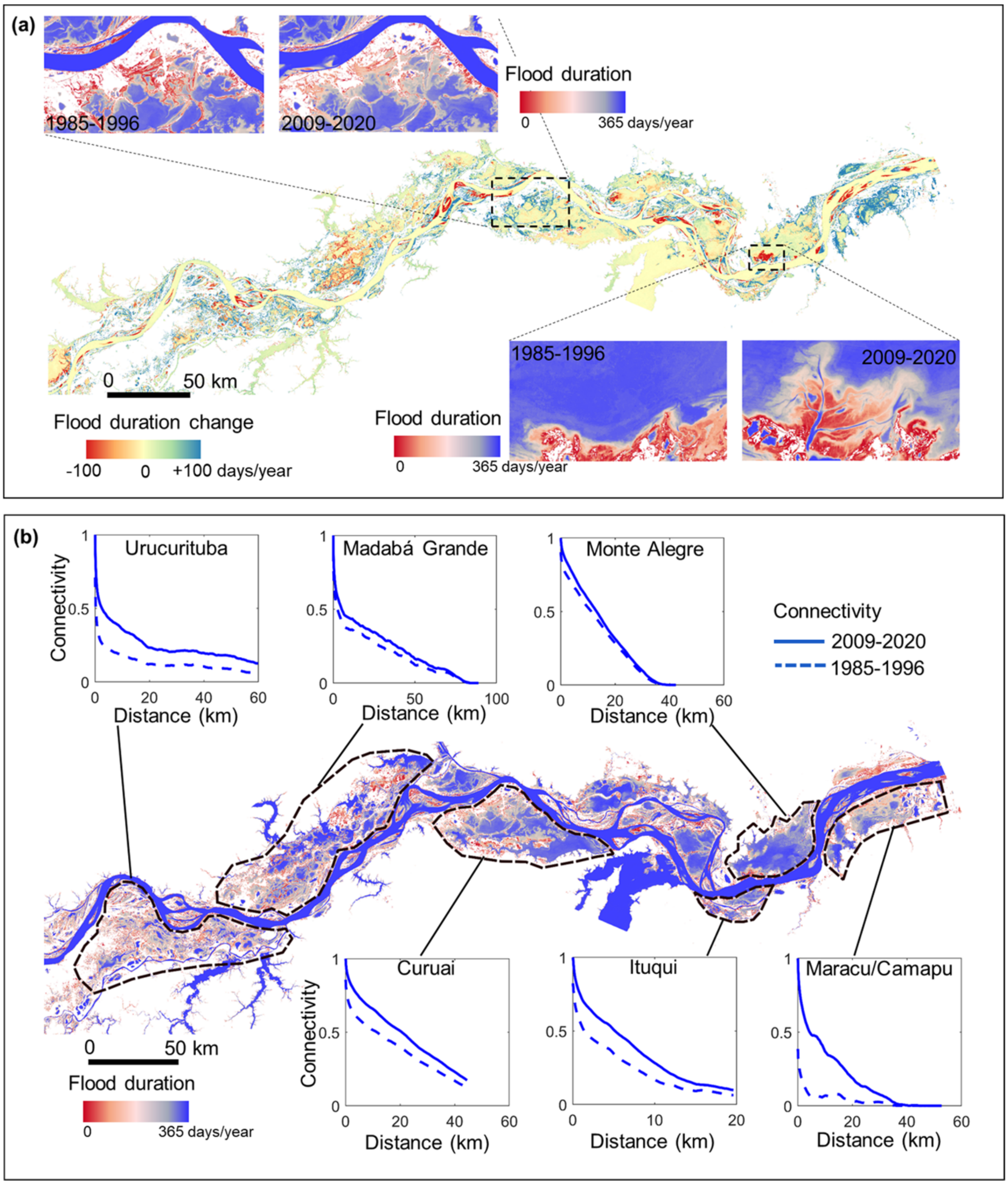

Figure 3. Increase of Amazon open water lateral connectivity and floodplain lake areas based on Landsat observations of open-water area. (a) Change in flood duration between 1985–1996 and 2009–2020 (the earliest and latest 11 year periods available with GSWO). Areas where flood duration has decreased are associated with floodplain sedimentary processes, as shown in the detail for a crevasse formation in the Lago Grande de Monte Alegre region. (b) Open water lateral connectivity increased in multiple Amazon floodplain regions in the last decade, in contrast to 1985–1996. The background map shows the mean annual flood duration for 2009–2020. In some locations, such as the Maracu and Camapu lakes, short distance connectivity has more than doubled. The degree of connectivity index refers to the number of pairs of open water pixels that are connected across a given distance. The values for each floodplain unit are divided by the maximum number of connected pairs for that particular unit.

(20%–40%) is observed in Curuai Lake, associated with its shoreline expansion, because most of the lake was already subject to flooding by 1986–1995. This increased connectivity can impact exchanges of water, sediments, nutrients, pollutants and organisms between the river and its floodplain (Junk *et al* 1989, Park and Latrubesse 2017). It is important to note that our analysis does not measure connections between areas with flooded vegetation due to GSWO limitations, and thus our result should be regarded as a lower bound for the increase in surface water connectivity.

4. Discussion

4.1. Multiple stressors affecting inundation regimes in a changing Amazon

While evidence of a shift to a novel hydroclimatic regime in the Amazon basin is mounting, climate projections remain uncertain about the net effects of climate change on river discharge, water levels, and floodplain inundation. Projections for the middle and end of this century suggest increased rainfall in the Amazon watersheds upstream from the Amazon-Purus confluence (Sorribas *et al* 2016, Zulkafli *et al* 2016, Brêda *et al* 2020). However, the propagation of these effects downstream to the mainstem Amazon and its floodplain is poorly understood. Changes in rainfall regimes are driven by complex ocean-atmosphere-land teleconnections, and it is uncertain the extent to which increased rainfall may be offset by decreases of rainfall and river discharges as projected for southern Amazon tributaries (Boisier *et al* 2015, Brêda *et al* 2020). Notably, our estimated 26% increase in the maximum inundation extent over 1980–2020 is considerably larger than late-century projections for the Peruvian Amazon (+18%), and much larger than projections for the central Amazon (+4%) (Sorribas *et al* 2016). Recent studies have shown that the drying of southern tributaries is leading to less area of open water in that region (Souza *et al* 2019). Along the Amazon mainstem floodplain, however, there is no evidence of a clear trend of increasing droughts (i.e. no negative trends either for minimum water levels, figure S2(b), or for annual minimum inundation extent, figure S3), even though parts of the Amazon have faced several extreme droughts in recent years (e.g. 2005 and 2010), particularly in the central-southern portion of the Amazon Basin. In some cases, droughts have occurred in the same year of an extreme flood along the mainstem river. This calls for more studies to understand spatial variation in the hydrological processes related to simultaneous occurrences of flood and drought events across this vast drainage basin (Ward *et al* 2020).

If sustained in the future, the increase in maximum inundation extent observed across the central Amazon floodplains, driven by a change in rainfall regime, is unlikely to be the only change affecting floodplain inundation regimes. Human-driven hydrological changes in the basin that potentially affect river discharge and floodplain inundation include construction of hydropower dams (Chaudhari and Pokhrel 2022), the development of industrial waterways in the western Amazon tributaries that require dredging of river channels (AIDESEP 2019), and deforestation in both the uplands and floodplains (Castello *et al* 2013). Understanding how these changes may interact either synergistically or antagonistically is important for planning dams and navigation channels as well as regulating deforestation. Furthermore, although our estimates based on hydrologic-hydrodynamic modeling considered a natural basin scenario, without the effects of anthropogenic impacts such as dams (Chaudhari and Pokhrel 2022, Flecker *et al* 2022), the impacts of rainfall changes on inundation extent reported here are well aligned with evidence from other, rainfall-independent remote sensing datasets. It is important to stress that such models have simplifications such as time-constant and rectangular river channel cross sections, which are necessary to be assumed due to scarcity of detailed, *in situ* data to be used in parameterization. However, their ability to simulate large-scale inundation extent and rainfall-runoff processes has been thoroughly investigated and is considered satisfactory (Yamazaki *et al* 2012, Paiva *et al* 2013, Siqueira *et al* 2018, Wongchuig *et al* 2019, Fleischmann *et al* 2022). Future developments in model parameterization, especially with improved information on floodplain topography (Yamazaki *et al* 2017, Fassoni-Andrade *et al* 2020), will further improve the accuracy of inundation extent estimation at local scales.

4.2. Environmental and social implications of increased flooding

Increases in the extent, duration and connectivity of floodplain inundation in the Amazon Basin have multifarious implications for floodplain ecosystems, geomorphological dynamics, biogeochemical processes, and the people who depend on floodplains. The exchange of sediment between floodplain lakes and the river channel is expected to intensify with increased flooding, as reported for the Curuai floodplain lake (Rudorff *et al* 2018). In addition to local geomorphological changes, increased floodplain sediment deposition could in turn lead to changes in the total sediment export to the ocean (Anthony *et al* 2021).

Fluxes of methane and carbon dioxide from aquatic habits to the atmosphere in the Amazon are large and dependent on inundated area and exchanges of nutrients and organic matter between rivers and floodplains (Richey *et al* 2002, Melack *et al* 2004, Abril *et al* 2014). Hence, these fluxes will likely increase with greater inundation. The role of wetlands in the increasing rates of global methane emission has been debated in the literature (Zhang *et al* 2017, Wilson *et al* 2020). While airborne observations from 2010 to 2018 suggest no clear trend in Amazon methane emissions (Basso *et al* 2021), the implications for methane emissions of the increased Amazon floodplain inundation require more study.

Increased inundation extent and duration are expected to affect fishes and fisheries yields, likely increasing fish production via increased feeding opportunities, growth, and recruitment (Welcomme 1985, Castello *et al* 2015). However, fish production also depends on primary production and the response of forest trees to a changing flood regime (Castello and Macedo 2016). Increased duration of inundation results in shorter dry periods, which can affect many floodplain plant and animal species (Castello and Macedo 2016) as well as the production of livestock and crops on the floodplains (Junk *et al* 2000), and may exacerbate fishing difficulties during high water levels, which is known to induce food insecurity for riverine human populations (Tregidgo *et al* 2020).

Although human populations along Amazonian floodplains have historically adapted to cope with and benefit from the annual flood pulse, recent extreme floods are driving migrations and negatively impacting disease risk, sanitation, mobility, and the transport of agricultural goods (Pinho *et al* 2015, Fonseca *et al* 2022). Adverse effects of flooding are particularly severe for vulnerable populations that depend on subsistence agriculture and that cannot readily move (Pinho *et al* 2015). A number of adaptive actions are being implemented to cope with increased floods, such as improving flood risk mapping in remote and urban areas, strengthening of civil defense, social programs for disaster preparedness and post-event response, and development of early warning systems (Marengo *et al* 2013, Pinho *et al* 2015). However, communication to remote rural communities regarding flood risk and development of adaptation strategies, such as pre-event food saving, agricultural water-resilient structures (e.g. floating planting beds) and crops, and temporary upland migration, remains challenging (Andrade *et al* 2017), as does the development of flood-resilient urban centers.

5. Conclusions

The Amazon River basin has been facing multiple extreme events in the last decade. Here, we used two hydrological models and multiple remote sensing datasets to investigate the changes in the inundation dynamics of the Amazon since 1980. Hydrological models show that since then the maximum inundation extent of the central Amazon floodplain has increased by 26%, or ∼25 000 km^2—an area equivalent to the size of Belgium. The Landsat-based GSWO dataset revealed increases in flooding duration and river-floodplain connectivity in the lower Amazon reaches, where multiple open water areas are common. Such changes have multiple consequences for floodplain ecosystems and the people that rely on them. Governments from local to national, as well as international organizations, must strengthen mitigation measures, particularly for vulnerable populations across the Amazon river-floodplain system. There is thus an urgent need to understand the changes, build resilience to their impacts, and mitigate their drivers to the extent possible.

Data availability statement

All data that support the findings of this study are included within the article (and any supplementary files).

Data and materials availability

All data used in this research are freely available, and described in the Materials and Methods section. *In-situ* river water level and discharge data from Brazilian National Water Agency are available at www.snirh.gov.br/hidroweb/, and from Peru's SENAMHI at www.senamhi.gob.pe/?p=pronostico-meteorologico. Documentation and outputs for the MGB and CaMa-Flood models are available at www.ufrgs.br/lsh/ and http://hydro.iis.u-tokyo.acjp/∼yamadai/cama-flood, respectively, and GSWO data are available at Google Earth Engine (more details at https://global-surface-water.appspot.com). CHIRPS rainfall is available at www.chc.ucsb.edu/data/chirps. GRACE data from JPL were obtained at https://podaac-tools.jpl.nasa.gov/drive/files/allData/tellus/L3/mascon/RL06/JPL/v02/CRI/netcdf.

Acknowledgments

The work was part of the SABERES project funded by the BNP Paribas Foundation as part of its 'Climate & Biodiversity Initiative' 2019 program, led by Dr Marie-Paule Bonnet. The authors acknowledge Dr David Kaplan, Dr David da Motta Marques, Dr Naziano Filizola and Dr Fernando Jaramillo for their collaboration on an earlier version of this manuscript.

Funding

CNPq (Conselho Nacional de Desenvolvimento Científico e Tecnológico, Brazil) Grant 141161/2017-5 (ASF)

CNES (SWOT-ST project SWOT for SOUTH AMERICA) Grant 6018-4500066497 (FP, MPB)

CNES SWOT-ST project SWOT Wetlands Hydrology Monitoring (FP, MPB)

IRD Groupement De Recherche International (GDRI) SCaHyLab (FP)

NASA IDS Grant NNX17AK49G (JMM)

US National Science Foundation (Division of Environmental Biology) Grant 1753856 (JMM)

NSF-Belmont Forum Award 1852113 (LC)

ANR and IRD Grant ANR-18-MPGA-0008 (AMANECER-MOPGA project) (SWC, JCE)

JSPS KAKENHI Grant 21H05002 (DY, MR)

BNP Paribas Foundation (SABERES Project - Climate & Biodiversity Initiative)

Author contributions

All authors contributed substantially to the work presented here.

Conceptualization: A S F, F P, S H, A F, S W, R P, J C E, E F C

Methodology: A S F, F P, S H, A F, S W, R P, J C E, D Y, M R

Investigation: A S F, F P, S H, A F, S W, R P, J C E, L C
Supervision: F P, R P, W C
Writing—original draft: A S F, F P, S H
Writing—review & editing: all authors

Conflict of interest

Authors declare that they have no competing interests.

ORCID iDs

Ayan S Fleischmann https://orcid.org/0000-0002-8547-4736
Fabrice Papa https://orcid.org/0000-0001-6305-6253
Stephen K Hamilton https://orcid.org/0000-0002-4702-9017
Alice Fassoni-Andrade https://orcid.org/0000-0002-3233-8781
Sly Wongchuig https://orcid.org/0000-0002-1116-0742
Jhan-Carlo Espinoza https://orcid.org/0000-0001-7732-8504
Rodrigo C D Paiva https://orcid.org/0000-0003-2918-6681
Etienne Fluet-Chouinard https://orcid.org/0000-0003-4380-2153
Rafael M Almeida https://orcid.org/0000-0001-5398-7054
Marie-Paule Bonnet https://orcid.org/0000-0002-3950-4041
Luna G Alves https://orcid.org/0000-0003-4362-3737
Dai Yamazaki https://orcid.org/0000-0002-6478-1841
Menaka Revel https://orcid.org/0000-0003-0390-8279
Walter Collischonn https://orcid.org/0000-0002-7630-396X

References

Abril G *et al* 2014 Amazon River carbon dioxide outgassing fuelled by wetlands *Nature* **505** 395–8

AIDESEP 2019 *Amazon Waterway: Good business for Perú? A legal, environmental and economic perspective on indigenous peoples* (available at: https://dar.org.pe/archivos/brief_waterway.pdf) (Accessed 17 Feb 2023)

Aires F, Prigent C, Fluet-Chouinard E, Yamazaki D, Papa F and Lehner B 2018 Comparison of visible and multi-satellite global inundation datasets at high-spatial resolution *Remote Sens. Environ.* **216** 427–41

Anthony E J, Brondizio E S, Dos Santos V F, Gardel A and Besset M 2021 Sustainable management, conservation, and restoration of the Amazon River Delta and Amazon-influenced Guianas coast: a review *Water* **13** 1–23

Barichivich J, Gloor E, Peylin P, Brienen R J W, Schöngart J, Espinoza J C and Pattnayak K C 2018 Recent intensification of Amazon flooding extremes driven by strengthened Walker circulation *Sci. Adv.* **4** eaat8785

Basso L S *et al* 2021 Amazon methane budget derived from multi-year airborne observations highlights regional variations in emissions *Commun. Earth Environ.* **2** 1–14

Bates P D, Horritt M S and Fewtrell T J 2010 A simple inertial formulation of the shallow water equations for efficient two-dimensional flood inundation modelling *J. Hydrol.* **387** 33–45

Beck H E, Van Dijk A I J M, Levizzani V, Schellekens J, Miralles D G, Martens B and De Roo A 2017 MSWEP: 3-hourly 0.25° global gridded precipitation (1979–2015) by merging gauge, satellite, and reanalysis data *Hydrol. Earth Syst. Sci* **21** 589–615

Boisier J P, Ciais P, Ducharne A and Guimberteau M 2015 Projected strengthening of Amazonian dry season by constrained climate model simulations *Nat. Clim. Change* **5** 656–60

Brêda J P L F, de Paiva R C D, Collischon W, Bravo J M, Siqueira V A and Steinke E B 2020 Climate change impacts on South American water balance from a continental-scale hydrological model driven by CMIP5 projections *Clim. Change* **159** 503–22

Castello L, Isaac V J and Thapa R 2015 Flood pulse effects on multispecies fishery yields in the lower Amazon *R. Soc. Open Sci.* **2** 150299

Castello L and Macedo M N 2016 Large-scale degradation of Amazonian freshwater ecosystems *Glob. Change Biol.* **22** 990–1007

Castello L, Mcgrath D G, Hess L L, Coe M T, Lefebvre P A, Petry P, Macedo M N, Renó V F and Arantes C C 2013 The vulnerability of Amazon freshwater ecosystems *Conserv. Lett.* **6** 217–29

Chaudhari S and Pokhrel Y 2022 Alteration of river flow and flood dynamics by existing and planned hydropower dams in the Amazon River Basin *Water Resour. Res.* **58** e2021WR030555

Chen J L, Wilson C R and Tapley B D 2010 The 2009 exceptional Amazon flood and interannual terrestrial water storage change observed by GRACE *Water Resour. Res.* **46**

Costa M H, Botta A and Cardille J A 2003 Effects of large-scale changes in land cover on the discharge of the Tocantins River, Southeastern Amazonia *J. Hydrol.* **283** 206–17

da Motta Paca V H, Espinoza-Dávalos G E, Moreira D M and Comair G 2020 Variability of trends in precipitation across the Amazon river basin determined from the CHIRPS precipitation product and from station records *Water* **12** 1244

De Andrade M M N, Bandeira I C N, Fonseca D D F, Bezerra P E S, de Andrade Á S and de Oliveira R S 2017 Flood risk mapping in the Amazon *Flood Risk Management* (Rijeka: InTech) p 13 (available at: www.intechopen.com/books/advanced-biometric-technologies/liveness-detection-in-biometrics)

Espinoza J C, Marengo J A, Schongart J and Jimenez J C 2022 The new historical flood of 2021 in the Amazon River compared to major floods of the 21st century: atmospheric features in the context of the intensification of floods *Weather Clim. Extrem.* **35** 100406

Espinoza J C, Ronchail J, Marengo J A and Segura H 2019a Contrasting North–South changes in Amazon wet-day and dry-day frequency and related atmospheric features (1981–2017) *Clim. Dyn.* **52** 5413–30

Espinoza J C, Sörensson A A, Ronchail J, Molina-Carpio J, Segura H, Gutierrez-Cori O, Ruscica R, Condom T and Wongchuig-Correa S 2019b Regional hydro-climatic changes in the Southern Amazon Basin (Upper Madeira Basin) during the 1982–2017 period *J. Hydrol. Reg. Stud.* **26** 100637

Fassoni-Andrade A C, Paiva R C D, Rudorff C M, Barbosa C C F and E M L D M N 2020 High-resolution mapping of floodplain topography from space: a case study in the Amazon *Remote Sens. Environ.* **251** 112065

Flecker A S *et al* 2022 Reducing adverse impacts of Amazon hydropower expansion *Science* **375** 753–60

Fleischmann A S *et al* 2020 Trade-offs between 1-D and 2-D regional river hydrodynamic models *Water Resour. Res.* **56**

Fleischmann A S 2021 Inundações em múltiplas escalas na América do Sul: de áreas úmidas a áreas de risco (South American floods across scales: from natural wetlands to human-water systems) (Federal University of Rio Grande do Sul) (available at: https://lume.ufrgs.br/handle/10183/236862)

Fleischmann A S *et al* 2022 How much inundation occurs in the Amazon River basin? *Remote Sens. Environ.* **278** 113099

Fonseca F, Worfarth-couto B, Santos A, Marinho R, Martinez J and Naziano F 2022 Hydrological scenarios and malaria incidence in the Amazonian context *Water* **14** 1283

Friedman A R, Bollasina M A, Gastineau G and Khodri M 2021 Increased Amazon Basin wet-season precipitation and river discharge since the early 1990s driven by tropical Pacific variability *Environ. Res. Lett.* **16** 034033

Funatsu B M, Le Roux R, Arvor D, Espinoza J C, Claud C, Ronchail J, Michot V and Dubreuil V 2021 Assessing precipitation extremes (1981–2018) and deep convective activity (2002–2018) in the Amazon region with CHIRPS and AMSU data *Clim. Dyn.* **57** 827–49

Funk C *et al* 2015 The climate hazards infrared precipitation with stations—a new environmental record for monitoring extremes *Sci. Data* **2** 1–21

Gloor M, Brienen R J W, Galbraith D, Feldpausch T R, Schöngart J, Guyot J L, Espinoza J C, Lloyd J and Phillips O L 2013 Intensification of the Amazon hydrological cycle over the last two decades *Geophys. Res. Lett.* **40** 1729–33

Haghtalab N, Moore N, Heerspink B P and Hyndman D W 2020 Evaluating spatial patterns in precipitation trends across the Amazon basin driven by land cover and global scale forcings *Theor. Appl. Climatol.* **140** 411–27

Hamilton S K, Sippel S J and Melack J M 2002 Comparison of inundation patterns among major South American floodplains *J. Geophys. Res.* **107** 1–14

Heerspink B P, Kendall A D, Coe M T and Hyndman D W 2020 Trends in streamflow, evapotranspiration, and groundwater storage across the Amazon Basin linked to changing precipitation and land cover *J. Hydrol. Reg. Stud.* **32** 100755

Hess L L, Melack J M, Affonso A G, Barbosa C, Gastil-Buhl M and Novo E M L M 2015 Wetlands of the lowland Amazon basin: extent, vegetative cover, and dual-season inundated area as mapped with JERS-1 synthetic aperture radar *Wetlands* **35** 745–56

Junk W J, Bayley P B and Sparks R E 1989 The flood pulse concept in river-floodplain systems *Can. Spec. Publ. Fish. Aquat. Sci.* **106** 110–27

Junk W J, Ohly J J, Piedade M T F and Soares M G M 2000 *The Central Amazon Floodplain: Actual Use and Options for a Sustainable Management* (Leiden: B Publishers)

Kendall M G and Gibbons J D 1975 *Rank Correlation Methods* (London: Griffin)

Landerer F W *et al* 2020 Extending the global mass change data record: GRACE follow-on instrument and science data performance *Geophys. Res. Lett.* **47** 1–10

Langill J C and Abizaid C 2020 What is a bad flood? Local perspectives of extreme floods in the Peruvian Amazon *Ambio* **49** 1423–36

Marengo J A, Borma L S, Rodriguez D A, Pinho P, Soares W R and Alves L M 2013 Recent extremes of drought and flooding in Amazonia: vulnerabilities and human adaptation *Am. J. Clim. Change* **2** 87–96

Marengo J A and Espinoza J C 2016 Extreme seasonal droughts and floods in Amazonia: causes, trends and impacts *Int. J. Climatol.* **36** 1033–50

Melack J M and Coe M T 2021 Amazon floodplain hydrology and implications for aquatic conservation *Aquat. Conserv.: Mar. Freshw. Ecosyst.* **31** 1029–40

Melack J M, Hess L L, Gastil M, Forsberg B R, Hamilton S K, Lima I B T and Novo E M L M 2004 Regionalization of methane emissions in the Amazon Basin with microwave remote sensing *Glob. Change Biol.* **10** 530–44

Neal J, Schumann G and Bates P 2012 A subgrid channel model for simulating river hydraulics and floodplain inundation over large and data sparse areas *Water Resour. Res.* **48** 1–16

Paiva R C D, Buarque D C, Clarke R T, Collischonn W and Allasia D G 2011 Reduced precipitation over large water bodies in the Brazilian Amazon shown from TRMM data *Geophys. Res. Lett.* **38**

Paiva R, Buarque D C, Collischonn W, Bonnet M P, Frappart F, Calmant S and Bulhões Mendes C A 2013 Large-scale hydrologic and hydrodynamic modeling of the Amazon River basin *Water Resour. Res.* **49** 1226–43

Pangala S R *et al* 2017 Large emissions from floodplain trees close the Amazon methane budget *Nature* **552** 230–4

Park E and Latrubesse E M 2017 The hydro-geomorphologic complexity of the lower Amazon River floodplain and hydrological connectivity assessed by remote sensing and field control *Remote Sens. Environ.* **198** 321–32

Pekel J, Cottam A, Gorelick N and Belward A S 2016 High-resolution mapping of global surface water and its long-term changes *Nature* **540** 418–22

Pettitt A N 1979 A non-parametric approach to the change-point problem *Appl. Stat* **28** 126

Pinho P F, Marengo J A and Smith M S 2015 Complex socio-ecological dynamics driven by extreme events in the Amazon *Reg. Environ. Change* **15** 643–55

Pontes P R M, Fan F M, Fleischmann A S, de Paiva R C D, Buarque D C, Siqueira V A, Jardim P F, Sorribas M V and Collischonn W 2017 MGB-IPH model for hydrological and hydraulic simulation of large floodplain river systems coupled with open source GIS *Environ. Model. Softw.* **94** 1–20

Renó V F, Novo E M L M, Suemitsu C, Rennó C D and Silva T S F 2011 Assessment of deforestation in the Lower Amazon floodplain using historical Landsat MSS/TM imagery *Remote Sens. Environ.* **115** 3446–56

Richey J E, Melack J M, Aufdenkampe A K, Ballester V M and Hess L L 2002 Outgassing from Amazonian rivers and wetlands as a large tropical source of atmospheric CO_2 *Nature* **416** 617–20

Rudorff C M, Dunne T and Melack J M 2018 Recent increase of river-floodplain suspended sediment exchange in a reach of the lower Amazon River *Earth Surf. Process. Landforms* **43** 322–32

Santos M J, Medvigy D, Silva Dias M A F, Freitas E D and Kim H 2019 Seasonal flooding causes intensification of the river breeze in the Central Amazon *J. Geophys. Res. Atmos.* **124** 5178–97

Schellekens J *et al* 2017 A global water resources ensemble of hydrological models: the eartH2Observe Tier-1 dataset *Earth Syst. Sci. Data* **9** 389–413

Sherman M, Ford J, Llanos-Cuentas A and Valdivia M J 2016 Food system vulnerability amidst the extreme 2010–2011 flooding in the Peruvian Amazon: a case study from the Ucayali region *Food Secur.* **8** 551–70

Sippel S J, Hamilton S K and Melack J M 1992 Inundation area and morphometry of lakes on the Amazon River floodplain, Brazil *Arch. Hydrobiol* **123** 385–400

Siqueira V A, Paiva R C D, Fleischmann A S, Fan F M, Ruhoff A L, Pontes P R M, Paris A, Calmant S and Collischonn W 2018 Toward continental hydrologic–hydrodynamic modeling in South America *Hydrol. Earth Syst. Sci.* **22** 4815–42

Sorribas M V, de Paiva R C D, Fleischmann A S and Collischonn W 2020 Hydrological Tracking Model for Amazon Surface Waters *Water Resour. Res.* **56**

Sorribas M V, Paiva R C D, Melack J M, Bravo J M, Jones C, Carvalho L, Beighley E, Forsberg B and Costa M H 2016 Projections of climate change effects on discharge and inundation in the Amazon basin *Clim. Change* **136** 555–70

Souza C M, Kirchhoff F T, Oliveira B C, Ribeiro J G and Sales M H 2019 Long-term annual surface water change in the

Brazilian Amazon Biome: potential links with deforestation, infrastructure development and climate change *Water* **11** 566
Tapley B D, Bettadpur S, Watkins M and Reigber C 2004 The gravity recovery and climate experiment: mission overview and early results *Geophys. Res. Lett.* **31** 1–4
Tregidgo D, Barlow J, Pompeu P S and Parry L 2020 Tough fishing and severe seasonal food insecurity in Amazonian flooded forests *People Nat*. **2** 468–82
Trigg M A, Michaelides K, Neal J C and Bates P D 2013 Surface water connectivity dynamics of a large scale extreme flood *J. Hydrol.* **505** 138–49
Ward P J *et al* 2020 The need to integrate flood and drought disaster risk reduction strategies *Water Secur.* **11** 100070
Welcomme R L 1985 *River Fisheries* FAO Technical Paper No. 262 (Rome) p 320
Wilson C, Chipperfield M, Gloor M, Parker R, Boesch H, McNorton J, Gatti L, Miller J, Basso L and Monks S 2020 Large and increasing methane emissions from Eastern Amazonia derived from satellite data, 2010–2018 *Atmos. Chem. Phys. Discuss.* **21** 1–38
Wongchuig Correa S, R C D D P, Espinoza J C and Collischonn W 2017 Multi-decadal hydrological retrospective: case study of Amazon floods and droughts *J. Hydrol.* **549** 667–84
Wongchuig S C, de Paiva R C D, Siqueira V and Collischonn W 2019 Hydrological reanalysis across the 20th century: a case study of the Amazon Basin *J. Hydrol.* **570** 755–73
Yamazaki D, de Almeida G A M and Bates P D 2013 Improving computational efficiency in global river models by implementing the local inertial flow equation and a vector-based river network map *Water Resour. Res.* **49** 7221–35
Yamazaki D, Ikeshima D, Tawatari R, Yamaguchi T, O'Loughlin F, Neal J C, Sampson C C, Kanae S and Bates P D 2017 A high-accuracy map of global terrain elevations *Geophys. Res. Lett.* **44** 5844–53
Yamazaki D, Kanae S, Kim H and Oki T 2011 A physically based description of floodplain inundation dynamics in a global river routing model *Water Resour. Res.* **47** 1–21
Yamazaki D, Lee H, Alsdorf D E, Dutra E, Kim H, Kanae S and Oki T 2012 Analysis of the water level dynamics simulated by a global river model: a case study in the Amazon River *Water Resour. Res.* **48** 1–15
Zhang Z, Zimmermann N E, Stenke A, Li X, Hodson E L, Zhu G, Huang C and Poulter B 2017 Emerging role of wetland methane emissions in driving 21st century climate change *Proc. Natl Acad. Sci. USA* **114** 9647–52
Zhou X, Prigent C and Yamazaki D 2021 Toward improved comparisons between land-surface-water-area estimates from a global river model and satellite observations *Water Resour. Res.* **57** e2020WR029256
Zulkafli Z, Buytaert W, Manz B, Rosas C V, Willems P, Lavado-Casimiro W, Guyot J L and Santini W 2016 Projected increases in the annual flood pulse of the Western Amazon *Environ. Res. Lett.* **11** 014013